

An investigation on optimizing the carbonation resistance of coal bottom ash concrete with its carbon footprints and eco-costs

Nitin Ankura, Navdeep Singh

Online Publication Date: 30 September 2023

URL: <http://www.jresm.org/archive/resm2023.825ma0719.html>

DOI: <http://dx.doi.org/10.17515/resm2023.825ma0719>

Journal Abbreviation: *Res. Eng. Struct. Mater.*

To cite this article

Ankura N, Singh N. An investigation on optimizing the carbonation resistance of coal bottom ash concrete with its carbon footprints and eco-costs. *Res. Eng. Struct. Mater.*, 2024; 10(1): 135-164.

Disclaimer

All the opinions and statements expressed in the papers are on the responsibility of author(s) and are not to be regarded as those of the journal of Research on Engineering Structures and Materials (RESM) organization or related parties. The publishers make no warranty, explicit or implied, or make any representation with respect to the contents of any article will be complete or accurate or up to date. The accuracy of any instructions, equations, or other information should be independently verified. The publisher and related parties shall not be liable for any loss, actions, claims, proceedings, demand or costs or damages whatsoever or howsoever caused arising directly or indirectly in connection with use of the information given in the journal or related means.



Published articles are freely available to users under the terms of Creative Commons Attribution - NonCommercial 4.0 International Public License, as currently displayed at [here](https://creativecommons.org/licenses/by-nc/4.0/) (the "CC BY - NC").

Research Article

An investigation on optimizing the carbonation resistance of coal bottom ash concrete with its carbon footprints and eco-costs

Nitin Ankur^a, Navdeep Singh^{*b}

Department of Civil Engineering, Dr BR Ambedkar National Institute of Technology, Jalandhar, India

Article Info

Abstract

Article history:

Received 19 July 2023

Accepted 26 Sep 2023

Keywords:

Concrete;

Carbonation;

Carbon footprints;

Compressive strength;

Eco-costs;

Microstructure

Energy from coal-fed thermal power plants is provided at the cost of the generation of coal ash. Coal bottom ash (CBA) is an ash generated in coal-fed power plants which is landfilled. Existing literature reports the potential of CBA as a replacement for Portland cement (PC) and natural fine aggregates (NFA) in concrete. Carbonation is an important durability parameter of concrete having fatal consequences at later ages if not estimated and controlled as it leads to corrosion in reinforcement. In the present study, experimental, microstructural, and statistical analysis along with life cycle assessment was performed to investigate the combined effect of two-hour grinded CBA (GCBA) as PC (10-30%) and raw CBA as NFA replacement (0-50%) on compressive strength and carbonation resistance. Accelerated carbonation tests were performed at an exposure of four weeks after 28 and 90 days of curing. Among CBA-based concrete mixes, concrete with 20% GCBA and 25% CBA (G20C25) reported higher compressive strength and carbonation depth owing to pozzolanic reactivity and filler effect of fine CBA particles. However, G20C25 resulted in comparable performance in comparison with the control mix in terms of strength and carbonation resistance. The findings of X-ray diffraction spectroscopy, scanning electron microscopy and Fourier transform infrared spectroscopy also validate the trends. The mathematical models derived for the carbonation resistance and strength were well-fitted. Multi-objective optimization recommended 21.5% GCBA and 29.8% CBA as the optimum amount that resulted in 20.08% and 19.40% lower carbon footprints and eco-costs compared to control mix.

© 2024 MIM Research Group. All rights reserved.

1. Introduction

The durability and sustainability assessment of concrete are key aspects in the production of concrete as it is the most consumed building material around the world. The majority of the constituents of concrete are dependent on natural resources for procurement [1]. Concrete is being utilized at a very rapid pace hence, the rate at which natural resources are depleted is much higher than the rate at which they are being replenished. The construction of new infrastructure is not only a concern, as poor durability performance of concrete also demands repair and retrofitting which also increases the demand for concrete. The need of the hour is to reduce the overburden on the natural resources and alternative constituents of concrete must be explored that can perform in tandem with concrete prepared with conventional ingredients. Numerous industrial waste has been investigated for the potential replacement of cement, fine aggregates, and coarse aggregates in concrete [2–12]. Recently, many industrial wastes like fly ash, silica fumes,

*Corresponding author: navdeeps@niti.ac.in

^a orcid.org/0000-0002-6530-0368; ^b orcid.org/0000-0002-4524-408X

DOI: <http://dx.doi.org/10.17515/resm2023.825ma0719>

Res. Eng. Struct. Mat. Vol. 10 Iss. 1 (2024) 135-164

slag, recycled concrete aggregates, etc. have been discovered as alternative cement and aggregates in concrete, and promising results have been stated worldwide [2,4–12]. The rise in the global population results in increasing demand for concrete as well. Hence, it is important to develop alternatives that are not only durable but also sustainable.

With the rise in population, the energy demand especially electricity is also rising. The majority of the world depends on coal-fed thermal power plants for electricity generation. It has been estimated that 47% of global electricity will be provided by coal-fed thermal power plants by 2030 [13,14]. It has also been expected that despite the world's focus on renewable energy resources, the dependency on coal-fed power plants will persist for the coming decades. The cost effective and surplus energy from coal-fed thermal power plants is provided at the cost of the generation of coal ash that pollutes the environment. Coal bottom ash (CBA) is one such ash that is generally landfilled and unlike fly ash is yet to be developed as a potential replacement for building materials. The CBA particles are heavy and settle at the foot of the combustion chamber. It constitutes around 20-30% of overall coal ash. Also, the concentration of heavy metals like Arsenic, Barium, Nickel, etc. is three to four times higher than permissible limits that make it unsafe for landfill. It has been estimated that around 100 million tons of CBA are annually dumped into various dumpsites [15]. Attempts have been made in recent years to develop CBA as a replacement of natural fine aggregate (NFA) and cement in concrete [16–24]. The CBA resembles the size of NFA due to its coarser size and has been studied as NFA replacement. Few studies also reported CBA as cement replacement after grinding CBA to obtain size similar to the cement particle [25–34].

The replacement of aggregates and cement with industrial waste is common practice now a day. However, satisfactory performance in terms of mechanical as well as durability parameters must be ensured. Durable and environment sustainable products is the need of hour not only in construction industry but other industries also [1,35]. The durability of concrete is also related to environmental impacts of concrete as less durable concrete demands more repair and retrofitting those further aids in to enhancement of impacts associated with the concrete. Among the durability of concrete, carbonation is an important property as carbonation poses serious threat to reinforcement of the structures [9,36,37]. Carbonation may have fatal consequences if not rectified on time. Carbonation tends to lower the pH of concrete resulting in decreasing the alkalinity of concrete and making reinforcing bars prone to corrosion. Carbonation is one of the key aspects that leads to deterioration of concrete structures. Extensive research has been carried out to study the influence of industrial waste based concretes on the carbonation resistance [37–41], however, research carried out on the carbonation behavior of CBA-based concrete is scarce.

It has been revealed that when CBA has been used as NFA replacement, the carbonation is not governed by diffusion theory i.e. carbonation depth depends on square root of exposure period, as porous CBA particles provides easy permeability to diffusing gases [42]. It has also been stated that the carbonation depth increases with increase in CBA content. Existing literature revealed that due to pore size densification by the fine particle of CBA, using 10% CBA as NFA replacement yields similar carbonation depth in CBA-based concrete when compared to conventional concrete [19,42–46]. At higher replacement levels, the presence of porous CBA leads to poor interlocking between the particles consequently increasing the carbonation depth. Also, CBA as PC replacement in CBA concrete resulted in better performance in terms of carbonation resistance than fly ash-based concrete. However, there is very limited research available of the carbonation resistance of CBA concrete where CBA has been used as cement replacement [33]. Also, the effect of combined replacement of grinded CBA and raw CBA as cement and NFA replacement respectively on carbonation resistance is yet to be explored.

1.1. Research Objectives and Significance

The brief review of the existing studies has been presented in the above sections and it can be interpreted that carbonation resistance and environmental impacts of CBA-based concrete where CBA has been used as joint replacement of cement and NFA is yet to be explored. Therefore, the prime objectives of the present investigations are:

- Investigating the potential of CBA to be use as dual replacement i.e. as PC replacement in grinded form (GCBA) and as NFA in raw form (CBA) in concrete.
- Maximizing the utilization of GCBA and CBA so as to attempt reduction in environmental impacts and the consumption of natural resources in concrete without significant reduction/compensation in compressive strength, microstructural characteristics and carbonation resistance of the designed concrete mixes.
- Determining the carbon footprints and eco-cost associated with the CBA based concrete so as to determine its sustainability potential and reduction in environmental impacts in comparison with the conventional concrete.

Based on the outcomes of the abovementioned objectives, a design mix for concrete prepared with GCBA and CBA can be proposed that will not only satisfy the structural requirements of a concrete but will also minimize the detrimental effects of conventional concrete on people and the environment.

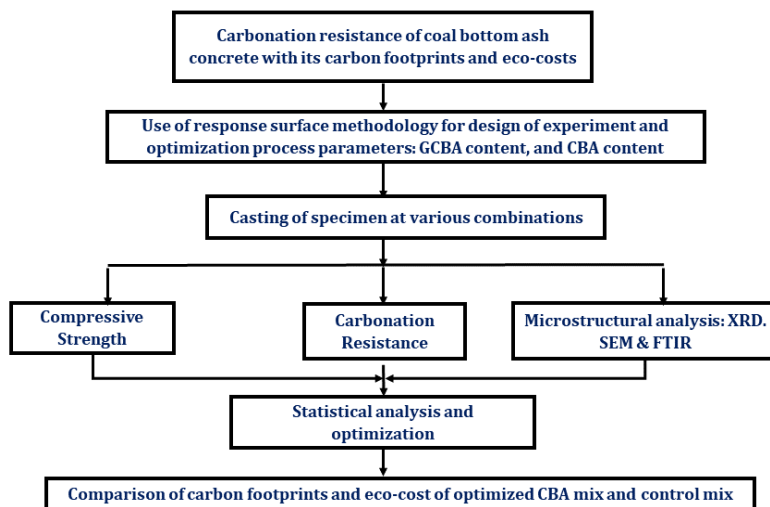


Fig. 1. Overview of the objectives and experimental program in the present study

The present research article can be divided in 4 parts where Part 1 contains present day scenario of coal combustion products along with a brief review of the existing literature on CBA based concrete. Part 2 contains materials and methods that are used in the present investigation for development of CBA based concrete. Part 3 contains results and discussions and provides in depth analysis of trends observed in compressive strength, carbonation depth, microstructural characteristics. Statistical analysis and optimization part has also been discussed in Part 3 along with the environmental impacts of CBA based concrete mixes. The research article concludes with key findings of the study in Part 4.

2. Materials and Methods

Fig.1 represents the overview of the objectives and experimental program of the present study. The present study focuses on investigating the effect of grinding CBA (2 hours), grinded CBA (GCBA) as Portland cement (PC) replacement and CBA as NFA replacement on carbonation resistance and environmental impacts of concrete. Accelerated carbonation tests along with compressive strength tests have been conducted to study the combined effect. Microstructure analysis like X-ray diffraction spectroscopy (XRD), scanning electron microscopy (SEM) and Fourier transform infrared spectroscopy (FTIR) were also performed to determine the influence of GCBA and CBA on microstructural characteristics. Statistical analysis was also performed to determine the significance of the GCBA, CBA and their interactions on the compressive strength as well as carbonations resistance. In addition, carbon footprints and eco-costs associated with CBA concrete were also calculated so as to determine the sustainability potential of CBA-based concrete.

2.1. Material

The present study used ordinary Portland cement (OPC) grade 43 for preparing concrete that conforms to IS 8112-2013 [47]. The natural coarse aggregate (NCA) of two different sizes i.e. 20 mm and 10 mm were used in 40:60 proportion conforming to IS 383 2016 [48]. The coarse sand conforming to zone II as per IS 383 2016 was used as natural fine aggregate (NFA). The physical properties of NFA and CBA are presented in Table 1.

Table 1. Chemical and Physical properties of PC, CBA, GCBA and NFA

Chemical composition of PC, CBA and GCBA			
Compounds	PC	CBA	GCBA
SiO ₂	20.89	56.4	56.5
Al ₂ O ₃	5.88	29.13	26.6
Fe ₂ O ₃	3.99	8.31	10.8
MgO	0.93	0.42	0.318
CaO	60.58	0.78	1.24
SO ₃	2.83	0.21	0.555
K ₂ O	1.12	1.27	1.48
Na ₂ O	0.81	0.07	0.24
TiO ₂	0.22	0.22	1.67
Loss of Ignition	2.01	0.87	-
Physical properties of NFA, CBA and GCBA			
Property	NFA	CBA	GCBA
Fineness Modulus (FM)	2.43	2.23	-
Water Absorption (%)	1.52	9.5	-
Specific Gravity	2.6	2.38	2.62
Specific Surface Area (m ² /g)	-	-	1.41
Average Pore Width (nm)	-	-	8.07
Pore Volume (cm ³ /g)	-	-	0.0024

Coal bottom ash (CBA) was acquired from Ropar thermal power plant and was utilized in two discrete ways i.e. in grinded form (GCBA) as a PC replacement and in raw form (CBA) as NFA replacement (Fig. 2). The CBA was grinded for 2 hours so as to obtain CBA at different specific surface area. A ball mill of 20 Kg capacity with 15 kg steel balls of varying diameter was used for grinding CBA at 55rpm.



Fig. 2. Coal bottom ash in (a) grinded form (b) raw form

The chemical composition of CBA along with the physical characteristic of GCBA are presented in Table 1. It is evident from Table 1 that the grinding of CBA has minimal effect on the chemical composition of CBA however, the particle size of CBA decreases significantly with grinding (Fig. 3). Table 1 also represents the specific surface area, average pore width, and pore volume for GCBA as obtained from Brunauer, Emmett and Teller (BET) test. Fig. 3 represents the particle size distribution curve for PC, GCBA, CBA and NFA and it can be interpreted that the particles of GCBA and CBA are finer than PC and NFA respectively. CBA also reported higher water absorption (9.5%) and lower specific gravity (2.38) than the NFA.

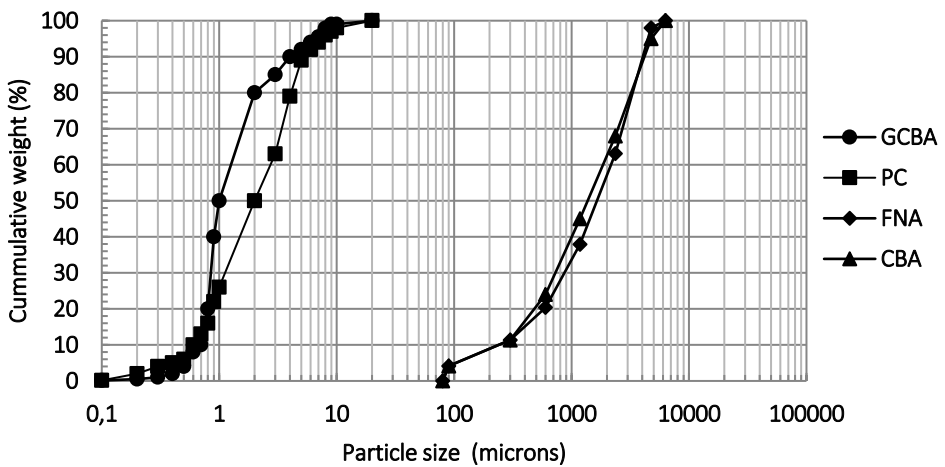


Fig. 3. Particle size distribution curves of GCBA, PC, CBA and NFA

2.2. Experimental Program

A two factor three level central composite design was adopted to study the combined effect of CBA as simultaneous replacement of PC and NFA in concrete. GCBA grinded for two hours was varied over the range of 10-20-30% replacement of PC whereas the effect of CBA was investigated over range of 0-25-50% replacement of NFA. A total of 9 concrete mixes of M 25 grade were cast as per IS 10262-2019 [49] and detailed mix proportion has been presented in Table 2.

Table 2. Mix proportions adopted for various CBA-based concretes

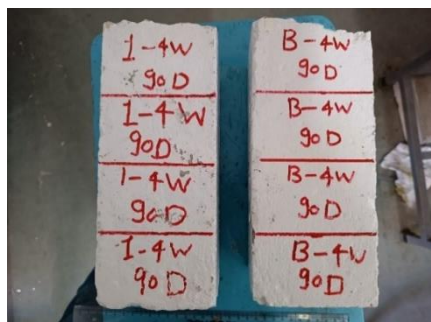
Mix	Grinding Period (Hours)	PC (kg/m ³)	GCBA (%)	GCBA (kg/m ³)	NFA (kg/m ³)	CBA (%)	CBA (kg/m ³)	NCA (kg/m ³)
Control	-	395	-	-	732	-	-	1068
G10C0	2	355.5	10	39.5	732	0	0	1068
G10C25	2	355.5	10	39.5	549	25	183	1068
G10C50	2	355.5	10	39.5	366	50	366	1068
G20C0	2	316	20	79	732	0	0	1068
G20C25	2	316	20	79	549	25	183	1068
G20C50	2	316	20	79	366	50	366	1068
G30C0	2	276.5	30	118.5	732	0	0	1068
G30C25	2	276.5	30	118.5	549	25	183	1068
G30C50	2	276.5	30	118.5	366	50	366	1068

A total of 4 responses were investigated i.e. 28 day and 90-day compressive strength, and carbonation depth after 28 day and 90 day of curing after 4 week of exposure to accelerated carbonation and are presented in Table 3. Compressive strength tests were performed on 100 mm cubes after 28 days and 90 days of curing conforming to IS 516:2006 [50]. After 28 days and 90 days of water curing, accelerated carbonation tests were performed on concrete mixes. Carbonation tests were performed on 500x100x100 mm beams that were split in two parts and covered with epoxy from 5 sides keeping one side exposed to accelerated carbon dioxide (CO₂). The samples were kept in accelerated carbonation chamber as present in Fig. 4. For the present study, the concentration of CO₂ was kept at 4% and the samples prepared were exposed to CO₂ for 4 weeks as per CPC-18, RILEM: 1988, EN 14360-2006 [51]. A solution containing 1% phenolphthalein in 70% ethyl alcohol was prepared and sprinkled on the slices. The colorless area represents the extent of carbonated area whereas pink color represents the non-carbonated area. Statistical analysis of these responses was also performed using analysis of variance (ANOVA). The microstructure characterization was performed using microstructure techniques such as X-ray diffraction (XRD), Scanning Electron Microscopy (SEM) analysis and Fourier Transform Infrared Spectroscopy (FTIR). Panalytical X'pert Pro (NDP) diffractometer was used for performing XRD analysis with 2θ in the range 5-80 degrees. Zeiss Sigma 500VP was used to study the SEM of the concrete mixes. FT-IR analysis was conducted on Bruker Tensor 27 FT-IR instrument.

The fast-track Life cycle assessment method was used to determine and compare the environmental impacts of optimized CBA concrete with conventional concrete. This innovative method was developed by Delft University of Technology and is an innovative and practical method for performing LCA [52]. The method is best suited for comparing the two different scenarios of a same product to determine the sustainability impacts metrics as this method generally focus on 'what to calculate' instead 'how to calculate' [52]. Carbon footprints and eco-costs were eco indicator selected for performing the LCA of optimized CBA concrete mix. The amount of greenhouse gases resulting from the production of material are represented in terms of carbon footprints and are calculated in kg CO₂ equivalent [52-57]. Eco-costs is monetized eco indicator that represents a virtual cost that need to be sustained so as to make the production of material sustainable and decrease the natural resource depletion and pollution to a level that resembles the carrying potential of Earth [52].



(a) Casted beams



(b) Beams painted with epoxy



(c) Beams placed in accelerated carbonation chamber



(d) Tested specimen

Fig. 4. Steps in determining the carbonation resistance of concrete

Table 3. Results of 28 and 90-day compressive strength and carbonation depth after 4 weeks of exposure

Std	Run	Mix	Factor 1 A: GCBA (%)	Factor 2 B: CBA (%)	Response 1 28 Day Compressive strength (MPa)	Response 2 90 Day Compressive strength (MPa)	Response 3 28 Day-4 Week Carbonation Depth (mm)	Response 4 90 Day-4 Week Carbonation Depth (mm)
-	-	Control	-	-	29.34	33.94	5	3
7	1	G20C0	20	0	25.87	33.09	5	1
6	2	G30C25	30	25	23.5	30.57	15	8
1	3	G10C0	10	0	23.04	28.774	14	6
9	4	G20C25	20	25	26.01	34.01	2	0
3	5	G10C50	10	50	20.14	27.12	7	5
2	6	G30C0	30	0	24.01	31.04	18	8
8	7	G20C50	20	50	24.29	32.01	8	5
5	8	G10C25	10	25	22.6	29.11	4	3
4	9	G30C50	30	50	21.57	27.6	29	14

3. Results and Discussion

3.1. Compressive Strength

The influence of 2-hour grinding, GCBA, and CBA on the compressive strength development of concrete has been presented in Fig. 5. It can be revealed that all the CBA-based concrete mixes yielded lower 28-day compressive strength than the control mix. This may be attributed to the inactive pozzolanic reactivity of GCBA particles that does not contribute in strength development in concrete at an early age. However, G20C25 reported a lower strength of 26.01 MPa in comparison with the control mix (29.34 MPa). Among CBA-based mixes, the 28-day compressive strength has been increased with an increase in GCBA content up to 20% and then decreased with a further increase in GCBA content to 30%. G20C0 yielded 12.25% and 7.7% higher compressive strength than G10C0 and G30C0. The compressive strength development tends to decrease with the increase in the GCBA (30%) due to the porous CBA particles that absorb the moisture and deters the hydration process. However, at 20% CBA, fine GCBA particles imparts pore filling effect that lead to increase in compressive strength after 28 days of curing [26,32].

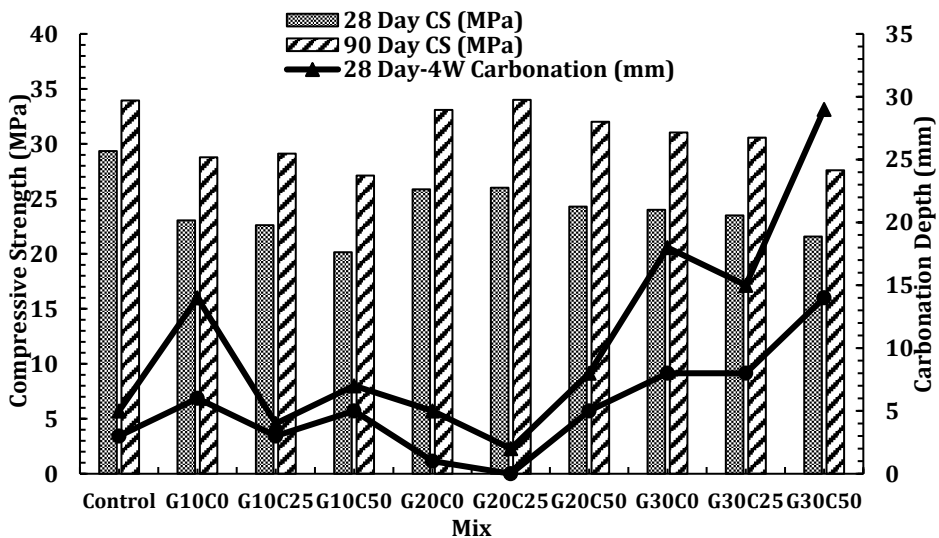


Fig. 5. Trends observed in 28-day compressive strength, 90-day compressive strength, 28 days- 4-week carbonation and 90 days-4-week carbonation

The increasing CBA percentage overall decrease the compressive strength development as shown in Fig. 5. For mixes prepared at 10 and 30% GCBA content, the compressive strength after 28-day curing decreased gradually with increase in CBA percentage as Mix G10C25 (22.6 MPa), G10C50 (20.14 MPa), G30C25 (23.5 MPa) and G30C50 (21.57) reported lower 28-day compressive strength than G10C0 (23.01 MPa) and G30C0 (24.0 MPa). However, Mix G20C25 reported higher but comparable 28-day compressive strength (26.01 MPa) as that of G20C0 (25.87 MPa). CBA as an NFA replacement imparts two distinctive effects; the refinement of pore size owing to fine CBA particles and the high porosity due to porous CBA particles. The pore size refinement effect dominates the effect of imparting high porosity up to 25% replacement resulting in higher compressive strength whereas, at a higher replacement level porous CBA particles result in the development of excess voids, thus, resulting in the drop in the 28-day compressive strength [17,58–63].

However, after 90 days of curing, the strength development in G20C25 was higher than the control mix. The compressive strength in G20C25 was 34.01 MPa in comparison with the

control mix that yielded a 90-day compressive strength of 33.91 MPa. The pozzolanic reactivity of GCBA particles along with the pore size refinement effect of CBA particles resulted in the formation of excess of calcium silicate hydrate (CSH) gel and dense microstructure in G20C25 that further resulted in enhancement in compressive strength. The overall behavior in CBA-based concrete was similar to 28-day strength wherein, the increase in GCBA and CBA replacement up to 20% and 25% respectively resulted in increase in compressive strength followed by gradual decrease in compressive strength with further increase in replacement.

3.2. Carbonation

Fig. 5 represents the trends observed in the carbonation depth of concrete mixes prepared with various replacement levels of GCBA and CBA. Fig. 6 illustrates the samples tested for carbonation after 28 day-4week and 90 day-4week exposure. It can also be revealed from Fig. 5 that after 28 days of curing and 4 week of exposure the carbonation depth in CBA-based concrete mixes was higher than the control mix. From Fig. 6, it can be interpreted that carbonated depth as shown by colorless region in the tested specimens was more in case of G10C0, G20C25 and G30C50 than the control mix. However, after 90 days of curing and 4 weeks of exposure, G20C25 yielded lower carbonation depth than the control mix. The lower carbonation depth in G20C25 can be revealed by comparing the carbonated depths as illustrated in Fig. 6. The pozzolanic reactivity of GCBA becomes active at the later stages and hence contribute in the production of CSH along with formation of dense microstructure that inhibits the moment of water and CO₂ in concrete.

Mix	28 Day – 4 Week Carbonation	90 Day – 4 Week Carbonation
Control		
G10C0		



Fig. 6. Carbonation depth as observed in various specimen of different concrete mix after 28 day-4-week carbonation and 90 day-4-week carbonation

Also, among the CBA-based concrete, the rate of carbonation decreased with increase in GCBA content at 20% and then further increased with increase in GCBA content after 28 and 90-day curing. Mix G20C0 yielded 2 mm carbonation and 1mm carbonation after 28 day-4week and 90 day-4week exposure respectively in comparison with G10C0 and G30C0 in which the carbonation depth was 5-1 mm and 8-5 mm after 28 day and 90-day 4 week of exposure. This may be due to pore densification by finer CBA particles and pozzolanic action of CBA that results in limiting the air permeability and hence, reduction in the carbonation depth. At lower percentage of GCBA (10%), the carbonation depth decreases with increase in CBA content as G10C25 (4-3mm) and G10C50 (7-5mm) reported lower carbonation depth than G10C0 (14-6mm) after 28 day-4 Week and 90 day-4-week exposure to accelerated carbonation. However, at higher replacement of GCBA (20%), the carbonation depth at 25% CBA is lower than 0% and 50% CBA content as G20C25 reported yielded 2 and 0 mm carbonation depth in comparison with G20C0 (5-1mm) and G20C50 (8-5mm) after 28 day-4 weeks and 90 day-4 week exposure. At 30% GCBA, the carbonation depth increases with increase in CBA content, though, the carbonation depth in G30C0 and G30C25 was almost comparable, whereas G30C50 yielded significant higher carbonation depth (29-14 mm) than G30C0 (18-8mm) and G30C25 (15-8mm) after 28 day-4 Week and 90 day-4 week exposure. The carbonation rate in CBA concrete increases due to porous CBA particles that increases the permeability of gases and accelerates the CO₂ diffusion into concrete. Poor interlocking between the particles of CBA and cement matrix may also lead to increase in carbonation depth.

3.3. Microstructural Analysis

3.3.1 X-Ray Diffraction (XRD) Analysis

The four concrete mixes i.e. D10C0, D20C25, D30C50 and control mix were analyzed for hydrated mineral phases using XRD analysis after 90 days of curing using Xpert high score. Several characteristics peaks of Portlandite ($\text{Ca}(\text{OH})_2$), Calcium silicate hydrate (CSH), and Ettringite (Aft) were identified at various d spacing and are plotted in Fig. 7. As the total count of Portlandite in G20C25 at d spacing 4.90 Å, 2.62 Å, 1.92 Å was 2589 lowest among control (2784), G10C0 (3463) and G30C50 (3538), therefore, it can be interpreted that Portlandite consumption was highest in the G20C25 and conversion of Portlandite to CSH was highest consequently resulting in higher compressive strength and lowest carbonation with respect to other mixes.

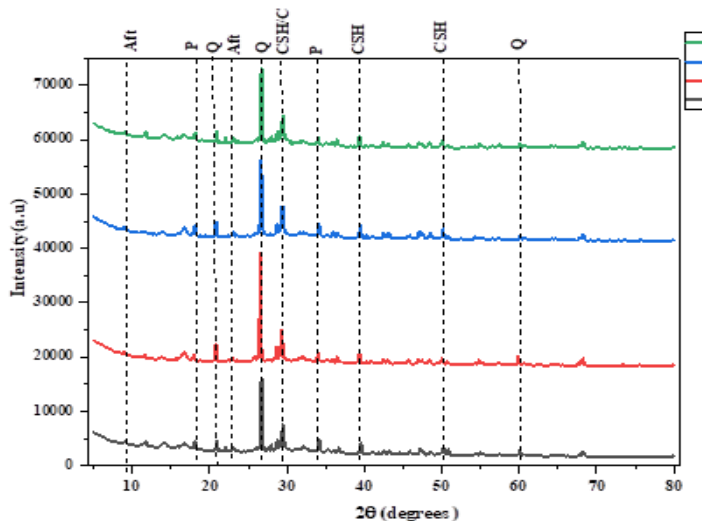


Fig. 7. XRD Spectrum for different concrete mix after 90 day of curing

Also, higher counts of CSH d spacing 3.04 Å, 2.72 Å, 1.82 Å in G20C25 than control mix, D10C0 and D30C25 further validated the trend observed in compressive strength and carbonation depth in CBA-based concretes. The presence of Ettringite (Aft) has also been detected in XRD spectrum and intensity was highest in G30C50 (875) followed by G10C0 (819), control mix (735) and G20C25 (702). The higher intensity of Aft in G30C50 also justified the lowest strength and maximum carbonation in the respective mix. The lean peaks of calcite were also detected that attributes to filler effect in cementitious matrix [64]. The existing literature also revealed the existence of these peaks in XRD spectrum analysis [9,65].

3.3.2 Scanning Electron Microscopy (SEM)

The microstructure of various concrete mixes was visualized and studied using SEM analysis. Fig. 8 represents the micrographs obtained for different concrete mixes after 90 days of curing. The presence of dense CSH can be revealed in micrographs of G20C25 as illustrated in Fig. 8 (c) which corroborated the attainment of highest compressive strength after 90 days and no carbonation after 4 weeks of exposure. The dense CSH gel offers higher resistance to compressive loads as well as ingress agents like water and CO_2 , hence results in excellent performance of concrete. The presence of excess of Ettringite has been revealed from micrograph presented in Fig. 8 (d) that validates the presence of high

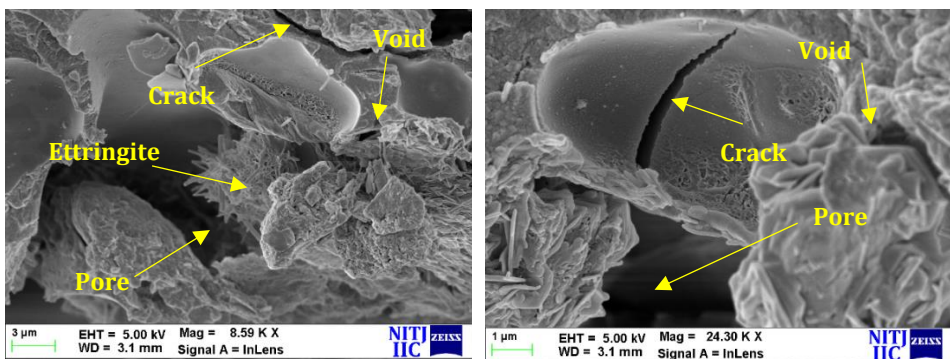
intensity Aft peak in XRD spectrum as well as the lowest compressive strength and maximum carbonation in G30C50. Fig. 8 (b) represents the micrographs for G10C0 and the presence of voids, cracks and Ettringite revealed lower compressive strength and higher carbonation depth in comparison with G20C25. These voids make concrete porous and provides easy passage to incoming water and CO_2 consequently leading to excessive carbonation. The micrographs of control mix are presented in Fig. 8 (a) shows the existence of dense CSH gel along with few traces of Ettringite as well as cracks along the ITZ that lead to lower but comparable strength in comparison with G20C25.

3.3.3 Fourier Transform Infrared Spectroscopy (FT-IR)

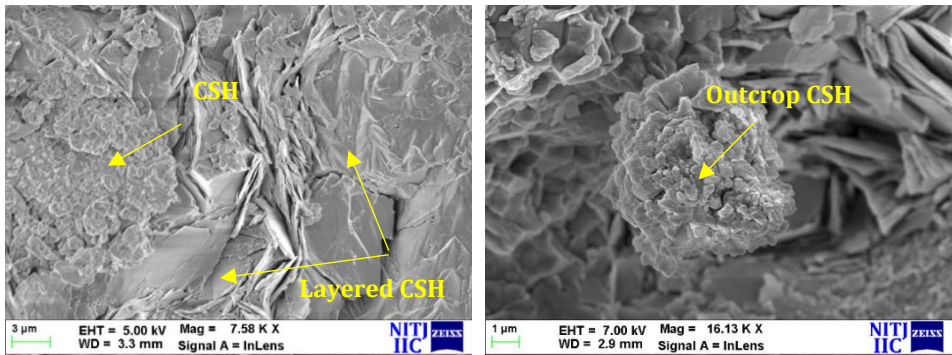
FT-IR analysis was performed to identify various functional groups present in different concrete mixes and presented in Fig. 9. The characteristics peak around wavenumber 3680 cm^{-1} , 2861 cm^{-1} , 1424 cm^{-1} , 1075 cm^{-1} , 955 cm^{-1} , and 887 cm^{-1} were produced in FTIR spectrum. The characteristic peak around 3680 cm^{-1} reveals the occurrence of Portlandite ($\text{Ca}(\text{OH})_2$) that originates from O-H stretching. The presence of CSH can be detected due to characteristic peak of Si-O originating from asymmetric bending around 955 cm^{-1} . The reaction between Portlandite and atmospheric carbon dioxide results in formation of intense peak around 1424 cm^{-1} and 887 cm^{-1} and confirmed the presence of carbonate (CO_3^{2-}). The sulphate group in ettringite has been observed around 1075 cm^{-1} .



(a) Control mix



(b) G10C0



(c) G20C25



(d) G30C50

Fig. 8. Micrographs for various concrete mix after 90 days of curing

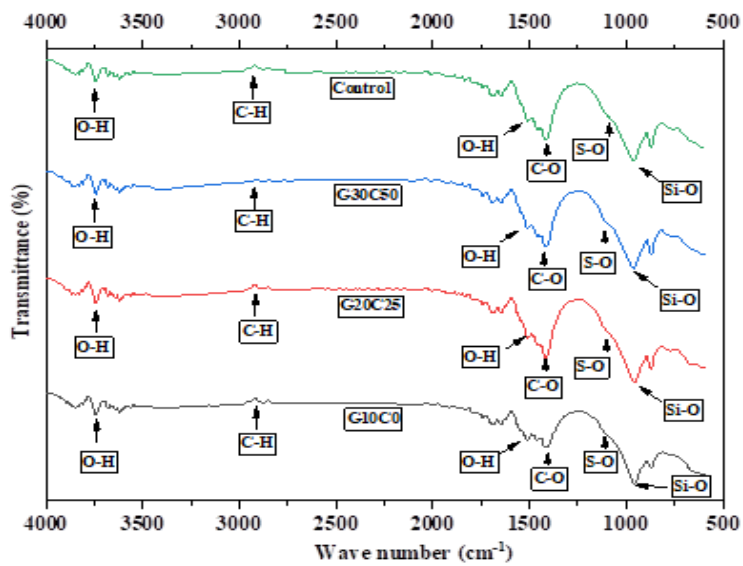


Fig. 9. FTIR spectrum for various concrete mix after 90 days of curing

From Fig. 9, it can be interpreted that the G20C25 exhibit a sharp and intense peak of Si-O as compared to other concrete mixes that further validates the formation of excess of CSH in the mix. The presence of dense CSH in G20C25 was also revealed in XRD and SEM analysis. More consumption of Portlandite in G20C25 has also been confirmed due to broader peak of O-H in comparison with control, D10C0 and D30C50. A steep bend in S-O as observed in G30C50 revealed the existence of higher amount of Ettringite than other mixes that resulted in significant reduction in compressive strength and increase in carbonation depth in the mix. The characteristics bands in the range 400-4000 cm^{-1} are in good agreement with the previous papers [11,66-70].

3.4. Statistical Analysis

Statistical analysis was done using regression analysis to analyze the compressive strength after 28 and 90 days of curing along with the carbonation depth after 4 weeks of exposure to accelerated carbonation in 28 and 90-day water cured specimen. Quadratic models were the best-found models for all the responses where p value lies below 0.05. Quadratic models were well fitted and no transformation was required. ANOVA was further used to check the significance of the models. Table 4 represents the results of ANOVA as obtained for 28-day compressive strength, 90-day compressive strength, 28 day-4-week carbonation depth and 90 day-4-week carbonation depth. Equations 1-4 represents the regression equations as obtained for the various responses investigated.

$$28 \text{ Day Compressive Strength} = +25.98 + 0.5480 A - 1.15 B + 0.1145 AB - 2.91 A^2 - 0.8813 B^2 \quad (1)$$

$$90 \text{ Day Compressive Strength} = +33.90 + 0.7010 A - 1.03 B - 0.4465 AB - 4.00 A^2 - 1.29 B^2 \quad (2)$$

$$28 \text{ Day-4 Week Carbonation Depth} = + 0.6667 + 6.17 A + 1.17 B + 4.50 AB + 9.50 A^2 + 6.50 B^2 \quad (3)$$

$$90 \text{ Day-4 Week Carbonation Depth} = + 0.1111 + 2.67 A + 1.50 B + 1.75 AB + 5.33 A^2 + 2.83 B^2 \quad (4)$$

The statistical significance of the model is determined using the F values which are generally the ratio of mean squares and reflect the ratio of explained variance to the unexplained variance. The F values for the 28-day compressive strength, 90-day compressive strength, 28 day-4-week carbonation depth and 90 day-4-week carbonation depth were 39.86, 36.43, 61.66, and 98.50 respectively, representing there are only 0.6%, 0.69%, 0.32% and 0.16% chance that larger F values than these in models can occur due to unexplained variations. The models are fitted satisfactorily as the $R^2(\text{adj})$ values of 0.96, 0.956, 0.974, and 0.983 for 28-day compressive strength, 90-day compressive strength, 28 day-4-week carbonation depth and 90 day-4-week carbonation depth respectively revealed that only 4%, 4.4%, 2.6%, 1.7% of the total variation that cannot be explained by the models. From the results of adequacy precisions, it can be concluded that design space can be navigated using the fitted models as the value were greater than 4 for all the responses. It can be revealed from Table 4 that A, B, A^2 , and B^2 are significant model terms for 28 days compressive strength as well as the 90 days compressive strength as p-values for these model terms were less than 0.05.

Table 4 also revealed that A, AB, A^2 , B^2 are significant model terms (p value < 0.05) for 28 day - 4 week carbonation depth whereas for 90 day-4 week carbonation the significant model terms were A, B, AB, A^2 , B^2 . Actual vs. Predicted plots were also found to determine the goodness of fit of the models and variations in the predicted values from the regressed diagonal line obtained from the actual values. It can be concluded from Fig. 10 (a and c)

and Fig. 11 (a and c) that residual points fall on regressed diagonal line throughout the range of actuals and hence, the adequacy of models can be established. Response surface plots were used to study the influence of GCBA and CBA along with their interactions on various responses studied. It can be revealed from slopes of response surface in Fig. 10 (b and d) that the compressive strength increases with the increase in GCBA and CBA content and then gradually decrease with further addition in replacement level. On contrary, slopes of response surface in Fig. 11 (b and d) validated that the carbonation depth decreases with the increase in GCBA and CBA content followed by gradual rise in carbonation depth with further addition of GCBA and CBA. The results in the current study are in good agreement with the existing studies that revealed similar pattern in compressive strength and carbonation depth in CBA-based concrete [19,21,26,30,32,33,71-75].

3.4.1 Optimization

A multi-objective optimization technique has been adopted in which response surface methodology serves as the base to find the optimal solution. Optimum setting of factors and responses were discovered using face central composite design method. The importance and weight along with the objective of optimization of factors as well as responses were defined so as to perform the objective based optimization. The optimization was carried out in Design expert software, that uses 'Desirability function' approach for executing optimization. In this method, desirability function for each response is constructed for carrying out the optimization. As presented in Table 5, 'Importance' is also assigned to individual factors and responses that can vary from 1 to 5. Value '5' is assigned for critical goals or goals having very high importance; value '3' is assigned for goals with medium or equal importance whereas value '1' is assigned for the goal with lowest importance. Since, the goals of maximising the replacement level of GCBA and CBA, maximising the compressive strength and minimising the carbonation depth as defined in multi-objective optimisation were considered to be equally important, hence a 'value of 3' was assigned by the authors. The 'value of 3' is also preferable as assigning any one goal the importance 'value of 5 or 1' makes the optimisation biased towards the assigned value of the goal. So, for practical point of view, the 'value of 3' delivers optimised results that further gives almost equal desirability to all the selected goals.

Each response is transformed into a dimensionless value called Individual desirability scale (di). The scale varies from 0 to 1, where 0 represents completely undesired response and 1 represents completely desired response. These individual transformations are combined using geometric mean that assists in examining the outcomes of various responses to form overall desirability (D). The method was first introduced by George Derringer & Ronald Suich in 1980 [76]. Though there are many other advanced methods that have been developed for multi objective optimization [77,78], the desirability function method has been widely used in existing studies [79-82] and hence the same methodology has been adopted in the present study.

Multiobjective optimization with desirability as mentioned in Table 5 has been performed in order to find the optimal combination of GCBA and CBA that would yield maximum compressive strength and minimum carbonation depth. The optimal solution as suggested by optimization revealed 21.51% GCBA and 29.82% CBA content as the best combination that will yield maximum strength with minimum carbonation. The desirability of factors and responses along with the total desirability of the optimization solution has been provided in Fig. 12. It can be revealed from Fig. 12 that the factors GCBA and CBA have the individual desirability of 0.57 and 0.58 whereas individual desirability for responses varied from 0.92 to 0.98.

Table 4. Results of ANOVA for 28-day compressive strength, 90-day compressive strength, 28 days-4-week carbonation and 90 days-4-week carbonation

28 Day Compressive Strength						90 Day Compressive Strength						
Source	Sum of Squares	df	Mean Square	F-value	p-value		Sum of Squares	df	Mean Square	F-value	p-value	
Model	28.34	5	5.67	39.86	0.0060	significant	45.45	5	9.09	36.43	0.0069	significant
A-GCBA	1.80	1	1.80	12.67	0.0378		2.95	1	2.95	11.82	0.0413	
B-CBA	7.98	1	7.98	56.11	0.0049		6.35	1	6.35	25.46	0.0150	
AB	0.0524	1	0.0524	0.3689	0.5865		0.7974	1	0.7974	3.20	0.1718	
A ²	16.95	1	16.95	119.24	0.0016		32.02	1	32.02	128.33	0.0015	
B ²	1.55	1	1.55	10.93	0.0455		3.33	1	3.33	13.36	0.0354	
Residual	0.4265	3	0.1422				0.7484	3	0.2495			
Cor Total	28.76	8					46.20	8				
Adjusted R ² = 0.960; Predicted R ² = 0.819; Adequacy Precision = 19.09						Adjusted R ² = 0.956; Predicted R ² = 0.805; Adequacy Precision = 16.12						
28 Day-4 Week Carbonation						90 Day-4 Week Carbonation						
Source	Sum of Squares	df	Mean Square	F-value	p-value		Sum of Squares	df	Mean Square	F-value	p-value	
Model	582.33	5	116.47	61.66	0.0032	significant	141.36	5	28.27	98.50	0.0016	significant
A-GCBA	228.17	1	228.17	120.79	0.0016		42.67	1	42.67	148.65	0.0012	
B-CBA	8.17	1	8.17	4.32	0.1291		13.50	1	13.50	47.03	0.0063	
AB	81.00	1	81.00	42.88	0.0072		12.25	1	12.25	42.68	0.0073	
A ²	180.50	1	180.50	95.56	0.0023		56.89	1	56.89	198.19	0.0008	
B ²	84.50	1	84.50	44.74	0.0068		16.06	1	16.06	55.94	0.0050	
Residual	5.67	3	1.89				0.8611	3	0.2870			
Cor Total	588.00	8					142.22	8				
Adjusted R ² = 0.974; Predicted R ² = 0.914; Adequacy Precision = 24.8						Adjusted R ² = 0.983; Predicted R ² = 0.927; Adequacy Precision = 32.19						
Cor Total: Corrected Total Sum of Squares, df : degree of freedom												

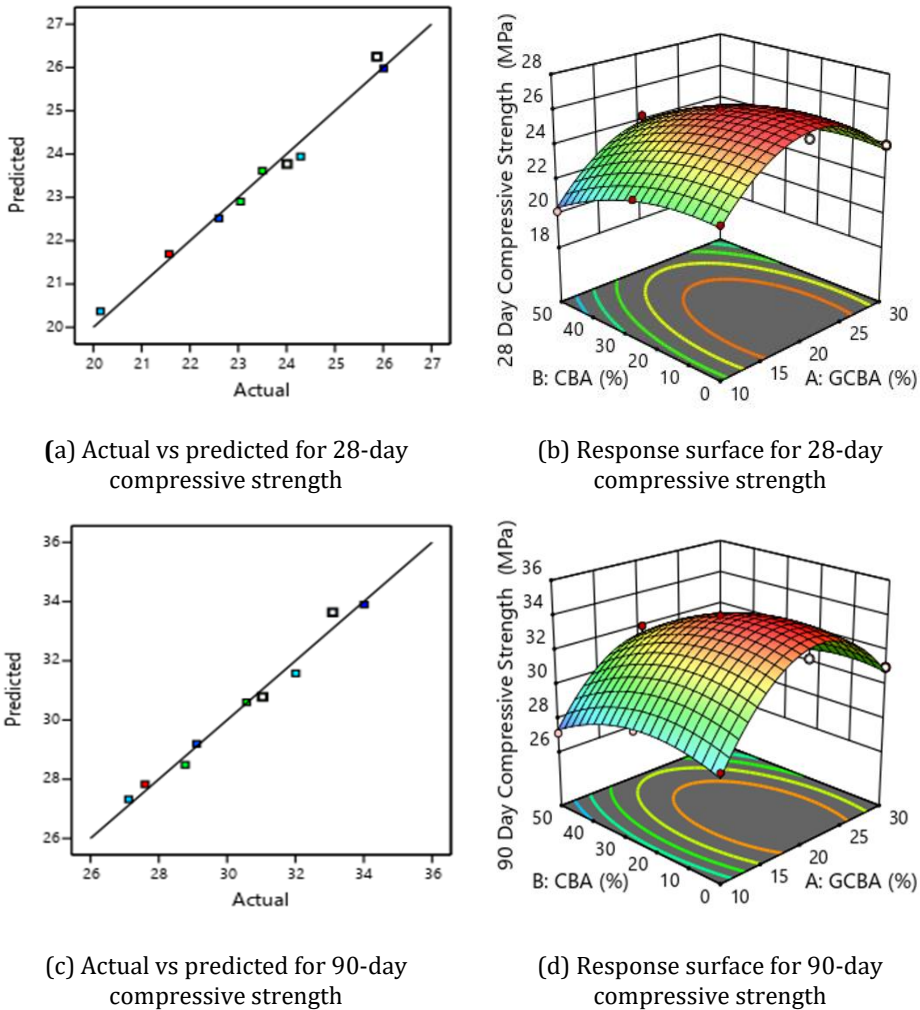
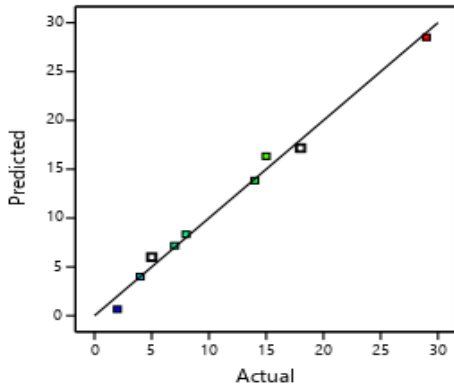
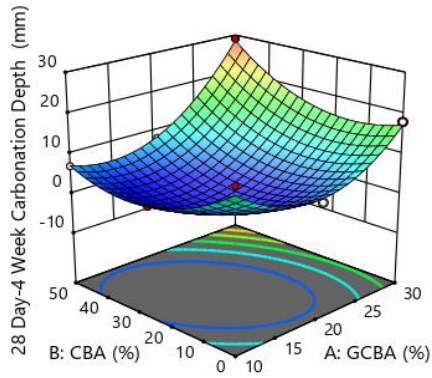


Fig. 10. Actual vs predicted and response surface graph for compressive strength after 28 days and 90 days curing

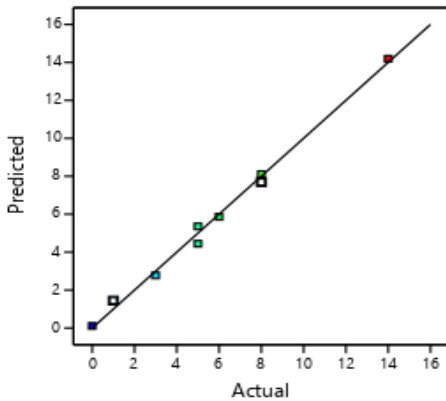
The contour plots for the responses were also obtained and are presented in Fig. 13. The suggested optimum combination of the GCBA and CBA was cast to validate the predicted values. The optimum combination yielded a 28-day compressive strength of 26.03 MPa in comparison with the predicted value of 25.773 MPa. The experimental result of the optimized combination correlated well with the predicted result and can be adopted as optimum mix combination while using CBA as a potential replacement of PC and NFA in concrete.



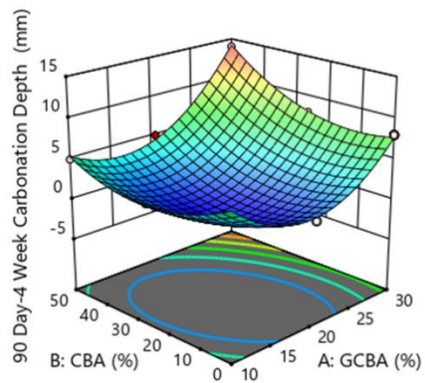
(a) Actual vs predicted for 28 day- 4 week carbonation



(b) Response surface for 28 day- 4 week carbonation



(c) Actual vs predicted for 90 day- 4-week carbonation



(d) Response surface for 90 day- 4-week carbonation

Fig. 11. Actual vs predicted and response surface graph for carbonation depths after 4 weeks of exposure to accelerated carbonation after 28 days and 90 days curing

Table 5. Desirability criteria adopted for optimization, and importance assigned to each investigated factor and response

Name	Goal	Lower Limit	Upper Limit	Lower Weight	Upper Weight	Importance
A:GCBA	maximize	10	30	1	1	3
B:CBA	maximize	0	50	1	1	3
28 Day Compressive Strength	maximize	20.147	26.01	1	1	3
90 Day Compressive Strength	maximize	27.12	34.01	1	1	3
28 Day-4 Week Carbonation Depth	minimize	2	29	1	1	3
90 Day-4 Week Carbonation Depth	minimize	0	14	1	1	3

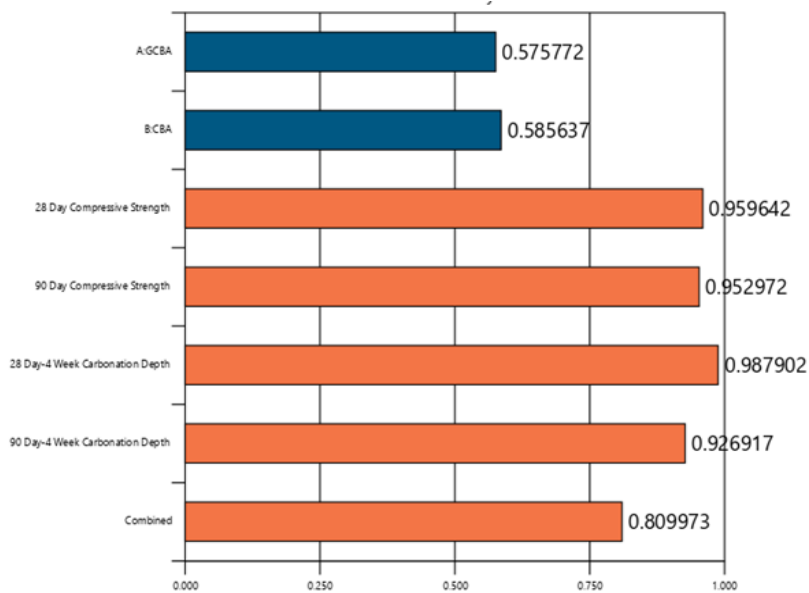


Fig. 12. Desirability of individual factors and responses along with overall combine desirability as obtained using desirability function approach

3.5. Life Cycle Assessment

The environmental impacts in terms of carbon footprints and eco-costs were calculated in order to compare the impacts associated with optimized concrete mix with conventional concrete mix. The optimization suggested 21.51% GCBA and 29.82% CBA content as the optimum content which is really encouraging in transforming traditional engineering design criteria considering function, cost and safety to more sustainable engineering design criteria that also considers impact on people and planet. Fast track life cycle assessment has been used to determine and compare the environment impacts of optimized CBA concrete with conventional concrete mix. The methodology adopted for performing Fast track LCA was in accordance with ISO 140040, 140044, and the LCA handbook of the ILCD [52,83–85].

3.5.1 Goal and Scope

The goal of conducting Fast track LCA was to determine the environmental impacts associated with optimized CBA-based concrete and compare it with conventional concrete mix so as to validate the benefits of utilizing the CBA in concrete over conventional concrete. An attempt has been made to enhance the environmental impacts of traditional concrete with the upcycling of CBA as a resource in concrete and reduce the burden on the natural resources from where majority of ingredients of concrete are acquired. 1 m³ of concrete was considered as the functional unit for performing the LCA. Fig. 14 represents the system boundaries adopted for performing 'Gate to Gate' LCA of optimized CBA concrete and control mix. The data sets compiled by Delft University of Technology were used to perform the LCA. Idemat 2023 database was referred for determining the eco impacts of various materials and processes involved in production of concrete [52].

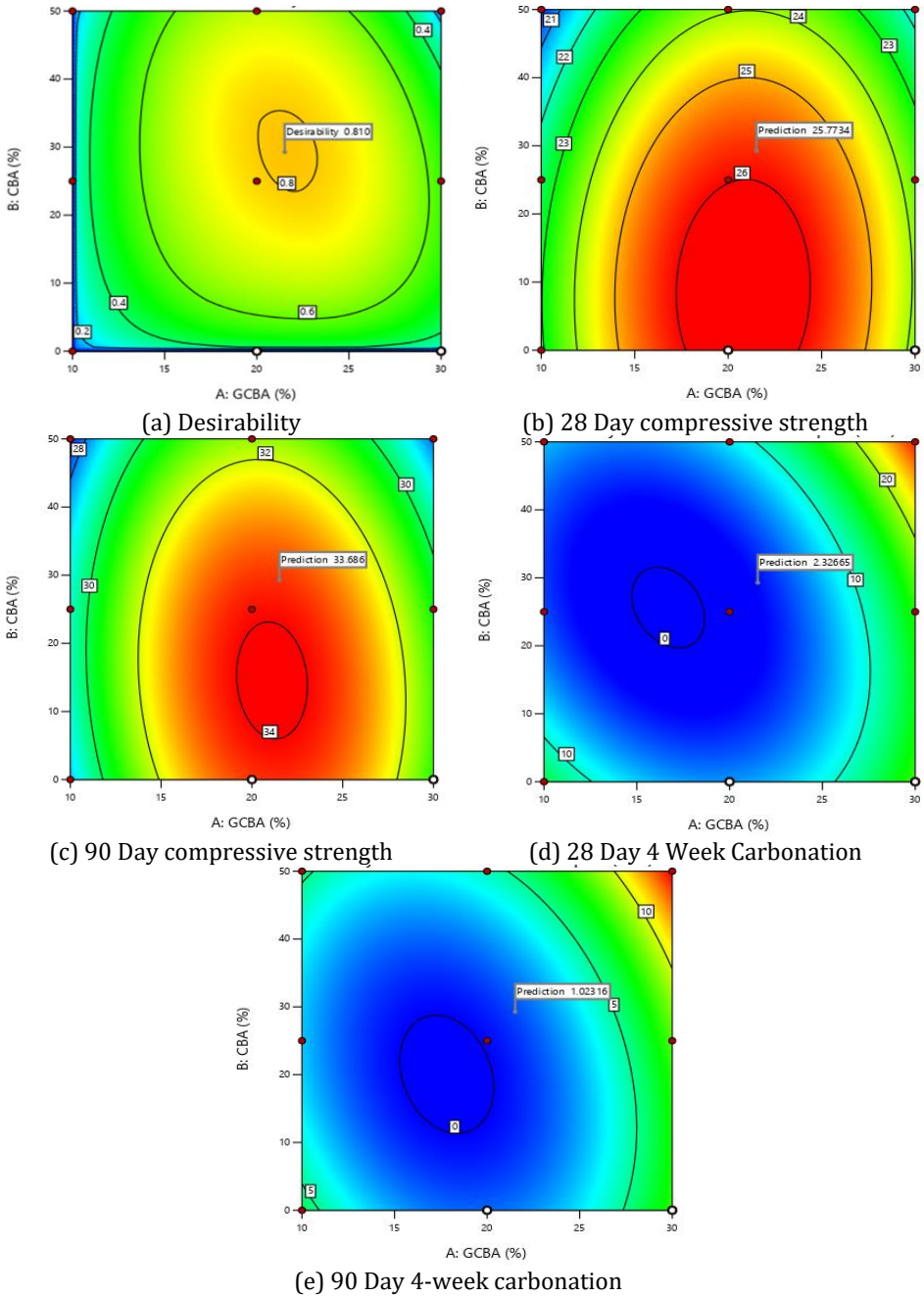


Fig. 13. Contour plots for optimized solutions

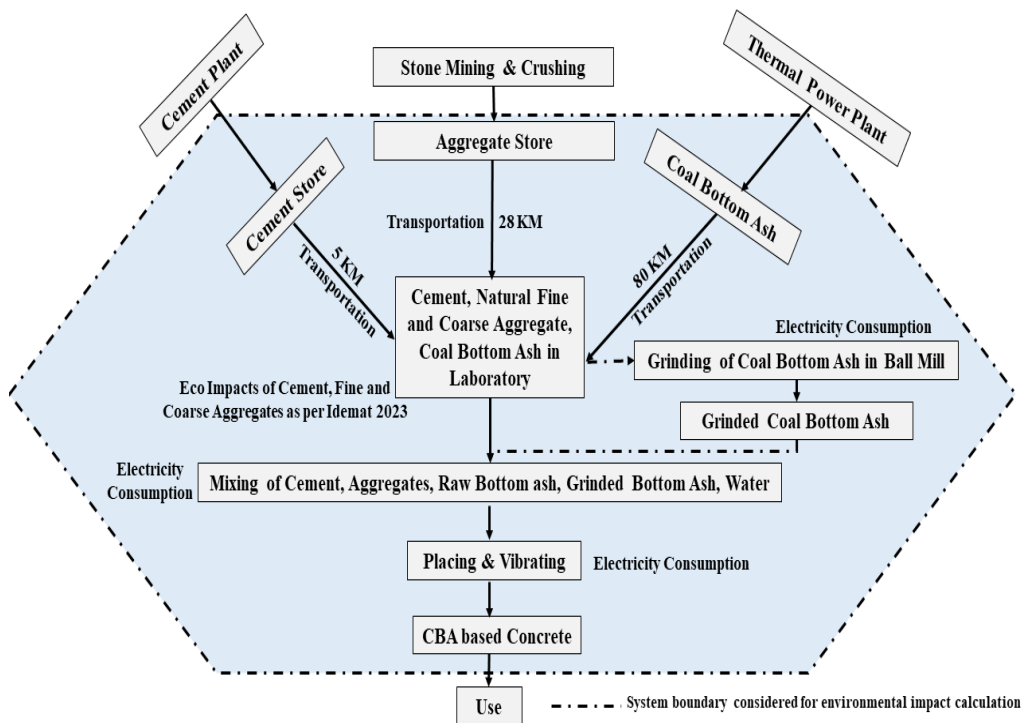


Fig. 14. System boundary considered in Gate-to-Gate life cycle assessment

3.5.2 Life Cycle Inventory Analysis

Inventory analysis was done under three broad categories as mentioned in the methodology of Fast track LCA i.e. Materials, Transportation, and Energy use. Since, the LCA in the present study considered only 'Gate to Gate' scenario, hence 'End of life' category was excluded from the inventory analysis. Table 6 compiled the various materials, transportation and energy use processes considered along with the life cycle inventory source. The 21.51% GCBA as PC replacement curtailed the cement content to 310 Kg per m^3 from 395 Kg per m^3 . The cement in both the scenario were purchased from same vendor and were transported over a distance of 5 KM. Similarly, the content of NFA was curtailed from 732 Kg/ m^3 to 517 Kg/ m^3 with 29.82% replacement of fine aggregate with CBA. The coarse aggregate content was 1068 in both the scenarios. The aggregates (NCA and NFA) were procured from same crusher and that required transportation over 28 KM. A total of 1800 Kg and 1585 Kg aggregates were transported over the specified distance. CBA was acquired from Ropar Thermal power plant and a total of 310 kg of CBA was transported over a distance of 80 KM. The impacts associated with transportation of CBA were only considered in optimized CBA concrete. GCBA was grinded for 2 hours in a ball mill in case of CBA-based optimized concrete mix, hence electricity consumption for grinding CBA was also included. The calculations and units' conversions adopted for determining the inventory analysis has been presented in Table 6.

3.5.3 Life Cycle Assessment

The excel sheet available on 'Sustainability Impact Metrics' website was used to perform the life cycle assessment and calculate carbon footprints as well as eco-costs associated with each step in manufacturing of conventional and optimized CBA concrete. Fig. 15 illustrates the total carbon footprints and eco-costs obtained from fast track LCA. A total

reduction of 21.519 % have been achieved in cement consumption in optimized CBA concrete as it yielded carbon footprint of 282.1 kg CO₂ equiv. in comparison with control mix that yielded carbon footprint of 359.45 kg CO₂ equiv. Also, carbon footprint associated with NFA in control mix is 1.464 kg CO₂ equiv. which was 29.317% higher than optimized CBA concrete (1.034 kg CO₂ equiv.). A total reduction of 21.645% has been reported in material stage of optimized CBA concrete mix as compared to normal control mix (Fig. 15). The reduction in cement content also reduced the carbon footprints associated with the transportation of cement wherein, cement transportation in optimized CBA concrete resulted in 21.229% lower carbon footprints (Fig. 15). The optimized concrete mix requires CBA which includes additional carbon footprints of 2.178 kg CO₂ equiv. with respect to control mix. Also, it can be revealed from Fig. 15 that lower aggregate content in optimized CBA concrete reduced the carbon footprints associated with transportation of aggregates. Total carbon footprints associated with transportation of aggregates reduced from 11.259 in case of control mix to 9.985 kg CO₂ equiv. in case of optimized CBA concrete. The carbon footprints associated with transportation stage increased by 7.57% in case of optimized concrete mix when compared with the control mix (Fig. 15). Similarly, optimized CBA concrete requires grinding of CBA that results in additional carbon footprints in comparison with the control mix. Control mix resulted in 0.283 kg CO₂ equiv. in energy use stage which was lower than the carbon footprints associated with optimized CBA concrete (1.0393 kg CO₂ equiv.). Overall, the carbon footprints associated with optimized CBA concrete was 303.06 kg CO₂ equiv. which were 20.08% lower than control mix (379.22 kg CO₂ equiv.).

Similarly, the eco-costs associated with cement consumption in optimized concrete mix was €49.6 which was 21.51% lower than the eco-costs of cement consumption in control mix (€63.2). Also, the lower consumption of fine aggregates resulted in 29.37% reduction in eco-costs associated with optimized CBA concrete (Fig. 15). A total reduction of 21.01% in eco-costs has been observed in material stage of optimized CBA concrete in comparison with control mix. In transportation stage, the transportation of CBA is an additional process that resulted in €0.717 more eco-costs in optimized concrete mix. Lower cement and fine aggregate content in optimized CBA concrete resulted in 22.03% and 11.32% lower eco-costs in comparison with the control mix. Grinding of CBA also resulted in additional eco-costs of €0.717 in optimized CBA concrete in comparison with control mix. Overall, the eco-costs associated with optimized CBA concrete was €55.415 which was 19.40% lower than control mix (€68.759).

Table 6. Life cycle inventory analysis for comparing the impacts associated with control mix and optimized CBA concrete

S No	Stage	Description	Impact Factor Considered	Unit	Eco-Impacts		LCI Source	Amount	
					Carbon Footprint (kg CO ₂ equiv./unit)	Eco-costs (€/unit)		Control Mix	Optimized CBA Concrete
1.	Materials	Cement	Idemat2023 Cement (Portland CEM I 52.5 N)	Kg	0.91	0.16	European reference Life Cycle Database (ELCD)	395.00	310
		Fine Aggregate	Idemat2023 Sand	Kg	0.002	0.001	Delft University of Technology based thesis (JG Vogtlander 2001)	732.00	517
		Coarse Aggregate	Idemat2023 Gravel	Kg	0.006	0.0016	Delft University of Technology based on Dutch Industry	1068.0	1068.00
		Water	Idemat2023 Drinking water Europe	Kg	0.001	0.0001	European reference Life Cycle Database (ELCD)	180.00	180.00
2.	Transport	Aggregates (From Quarry to Lab)	Idemat2023 Tractor (240 pk)	tkm	0.225	0.06	ELCD	1800 Kg transported for 28 Km = 50.04	1585 Kg transported for 28 Km = 44.380
		Cement (From Distributor to Lab)	Idemat2023 Truck+trailer 24 tons net (min weight/volume ratio 0.32 ton/m ³) (tkm)	tkm	0.091	0.03		395 Kg transported for 5 Km = 1.97	310 Kg transported for 5 Km = 1.550
		Coal bottom ash (From Thermal Power Plant to Lab)		tkm	0.091	0.03	Idemat Database	-	299.28 Kg transported for 80 Km = 23.942
3.	Use	Electricity (Concrete Mixing, Vibrating and other Operations)	Idemat2023 Electricity General	MJ	0.141	0.02	Idemat Database	3 HP motor run for 15 min = 2.01	3 HP motor run for 15 min = 2.01
		Electricity (Grinding of CBA)	Industry	MJ	0.141	0.02		-	1 HP motor run for 2 hours = 5.364

Adopted Unit Conversions: 1HP = 0.745 Kwh; 1Kwh = 3.6 MJ; 1 Kg for 1 Km = 0.001 tkm

3.5.4 Interpretation

The prime objective of the research was to obtain at comparable or at least at par performance of CBA-based concrete with respect to control mix in terms of compressive strength and carbonation resistance. Herein, it is important to mention that more concern was in maximizing utilization of coal ashes/bi-products (in form of GCBA and CBA) so as to reduce environmental impacts and the consumption of natural resources without significant reduction/compensation in strength and durability of the designed concrete mixes. It is further important to mention that GCBA/CBA mixes (5 out of 9 in total i.e., mixes G20C0, G20C25, G20C25, G30C0, and G30C25) made in this study resulted in compressive strength more than 30 MPa (as original mix was designed for a target strength of at least 25 N/mm²). Such grades of concrete can be successfully used for both structural and non-structural construction works.

Since considerable reductions in carbon footprints (20.08%) and eco-costs (19.40%) were observed as per the fast-track LCA, it can be inferred that the use of CBA as a potential cement and NFA substitute is an environmentally friendly sustainable alternative. Lack of significant impact on compressive strength has been rewarded with added advantage of significant reduction in the environmental impacts of CBA based concrete on comparing with the control mix. In comparison to the control mix, the CBA-based ideal concrete mix produced comparable mechanical and durability performance in terms of strength and carbonation resistance, and had less negative environmental effects. However, utilizing more effective milling parameters, such as increasing ball mill revolutions, ball mill feed, and shortening the optimal time for grinding CBA, can reduce the increased carbon footprints and eco-costs related to grinding CBA.

4. Conclusions and Future Work

The present investigation studied and optimized the compressive strength and carbonation resistance in CBA-based concrete wherein the effect of 2-hour grinding of CBA, GCBA as PC and CBA as NFA replacement was considered. The GCBA as PC replacement lead to increase in compressive strength and carbonation resistance at 20% replacement followed by a reduction in strength at 30% replacement. The pozzolanic reactivity of GCBA becomes active at later stages that leads to development of excess CSH and dense microstructure, consequently leading to enhancement in strength at later stages. The CBA as NFA replacement resulted in an enhancement in compressive strength and carbonation resistance till 25% replacement owing to the ascendancy of the pore size refinement effect. At higher replacement (beyond 25%), the porous CBA particles resulted in excess water absorption as well as porous microstructure leading to the formation of excess voids in concrete, consequently resulting in a reduction in the strength as well as carbonation resistance. XRD spectrum revealed higher count intensity of Portlandite and calcium silicate hydrate gel in G20C25. SEM analysis revealed dense cement matrix and interfacial transition zone (ITZ) formation in G20C25. FT-IR spectroscopy also governed the higher strength development and carbonation resistance at 20% GCBA and 25% CBA content, as broader peak of O-H bending and sharp-intense peak of Si-O was observed in G20C25 when compared to control and CBA-based concrete. The mathematical models obtained for compressive strength and carbonation depth strength are well fitted and are in good agreement with experimental as well as predicted values. 21.51% GCBA and 29.82% CBA are the optimum values of the factors that have combined desirability of 0.80 in achieving the desired compressive strength and carbonation resistance.

A reduction of 20.08% and 19.40% in carbon footprints and total eco-costs with the inclusion of 21.51 % GCBA and 29.82% CBA as PC and NFA replacement in concrete has been revealed in fast-track life cycle assessment.

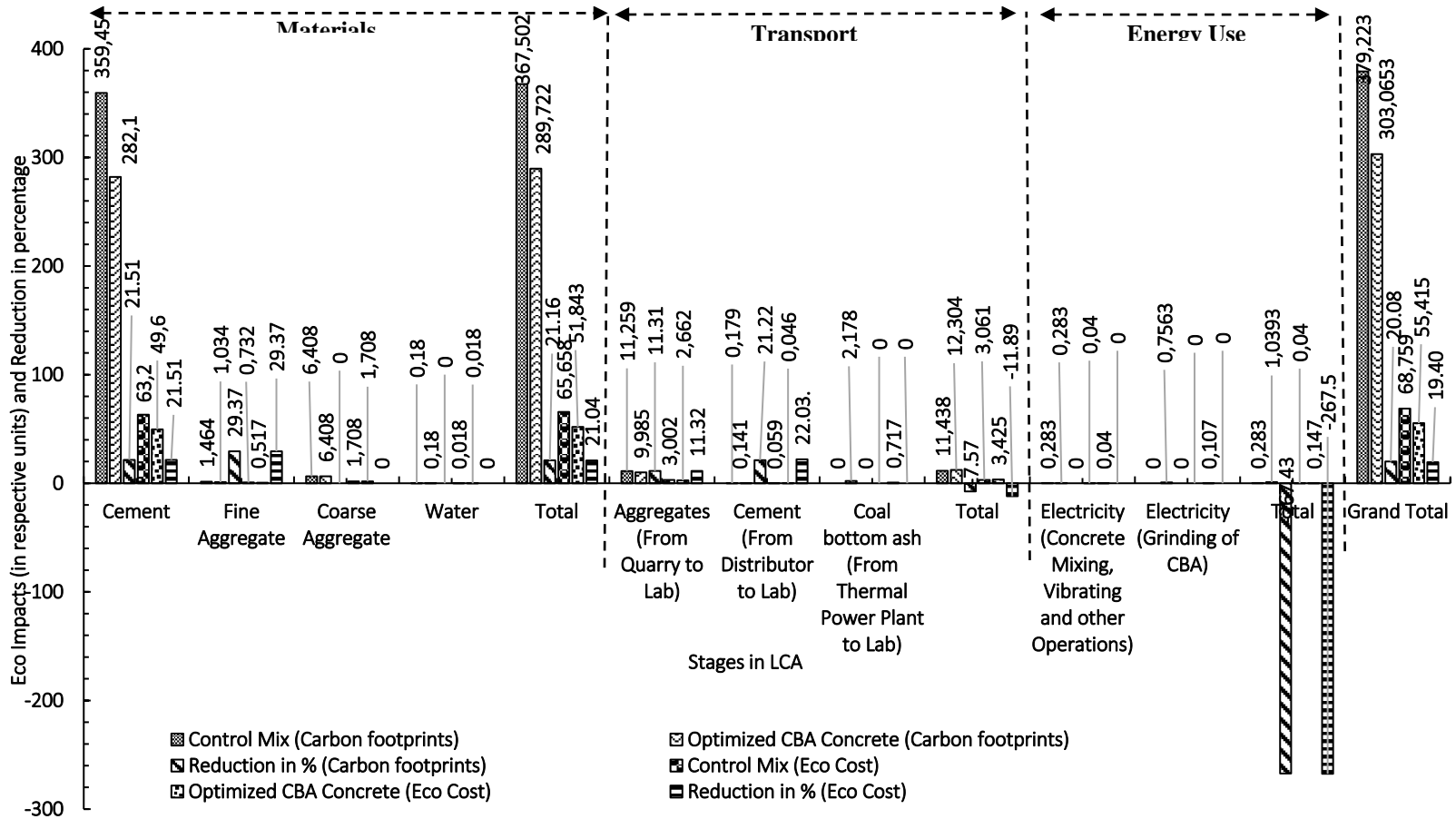


Fig. 15. Results of fast track life cycle assessment at various stages in production of CBA-based concrete and control mix

Based on the optimized values of the factors studied, a design mix for concrete prepared with GCBA and CBA can be proposed that will not only satisfy the structural requirements of a concrete but will also minimize the detrimental effects of conventional concrete on people and the environment. However, the grinding period of GCBA can be optimized further using more efficient milling factors like increase in revolutions of ball mill, increase in ball mill feed, etc. Also, reducing the water absorption of CBA is still a major concern and various chemical and physical treatment must be investigated to overcome the excessive water absorption. With these improvements, higher replacement of PC and NFA can be targeted without compromising the mechanical, durability and environmental aspects of CBA-based concrete.

Acknowledgement

The fellowship sponsored by the Ministry of Education, New Delhi to the first author is acknowledged. The author also acknowledges the Institute Instrumentation Centre (IIC), Dr B R Ambedkar National Institute of Technology Jalandhar India for providing microstructural testing facilities.

References

- [1] Ankur N, Singh N. A review on the life cycle assessment phases of cement and concrete manufacturing. In: Role of Circular Economy in Resource Sustainability. Springer, Cham; 2022. p. 85–96.
- [2] Boubekeur T, Boulekbache B, Aoudjane K, Ezziane K, Kadri EH. Prediction of the durability performance of ternary cement containing limestone powder and ground granulated blast furnace slag. *Constr Build Mater* . 2019;209:215–21. <https://doi.org/10.1016/j.conbuildmat.2019.03.120>
- [3] Singh N, Singh A, Ankur N, Kumar P, Kumar M, Singh T. Reviewing the properties of recycled concrete aggregates and iron slag in concrete. *J Build Eng* . 2022;60(May):105150. <https://linkinghub.elsevier.com/retrieve/pii/S2352710222011573>
- [4] Baite E, Messan A, Hannawi K, Tsohnang F, Prince W. Physical and transfer properties of mortar containing coal bottom ash aggregates from Tefereyre (Niger). *Constr Build Mater* . 2016;125:919–26. <http://dx.doi.org/10.1016/j.conbuildmat.2016.08.117>
- [5] Lau CK, Rowles MR, Parnham GN, Htut T, Ng TS. Investigation of geopolymers containing fly ash and ground-granulated blast-furnace slag blended by amorphous ratios. *Constr Build Mater*. 2019;222:731–7.
- [6] Corinaldesi V, Mazzoli A, Siddique R. Characterization of lightweight mortars containing wood processing by-products waste. *Constr Build Mater* . 2016;123:281–9. <http://dx.doi.org/10.1016/j.conbuildmat.2016.07.011>
- [7] Muthusamy K, Hafizuddin RM, Yahaya FM, Sulaiman MA, Syed Mohsin SM, Tukimat NN, et al. Compressive strength performance of OPS lightweight aggregate concrete containing coal bottom ash as partial fine aggregate replacement. In: IOP Conference Series: Materials Science and Engineering. 2018. p. 012099.
- [8] Dash MK, Patro SK, Rath AK. Sustainable use of industrial-waste as partial replacement of fine aggregate for preparation of concrete – A review. *Int J Sustain Built Environ* . 2016;5(2):484–516. <http://dx.doi.org/10.1016/j.ijsbe.2016.04.006>
- [9] Singh N, Nassar RUD, Kaur S, Bhardwaj A. Microstructural characteristics and carbonation resistance of coal bottom ash based concrete mixtures. *Mag Concr Res*. 2020;
- [10] Singh R, Patel M. Strength and durability performance of rice straw ash-based concrete: an approach for the valorization of agriculture waste. *Int J Environ Sci Technol*. 2022

- [11] Meena A, Singh N, Singh SP. High-volume fly ash Self Consolidating Concrete with coal bottom ash and recycled concrete aggregates: Fresh, mechanical and microstructural properties. *J Build Eng*. 2023;63(PA):105447. <https://doi.org/10.1016/j.jobe.2022.105447>
- [12] Rodríguez-Álvaro R, González-Fontebo B, Seara-Paz S, Rey-Bouzón EJ. Masonry mortars, precast concrete and masonry units using coal bottom ash as a partial replacement for conventional aggregates. *Constr Build Mater*. 2021;283.
- [13] Muthusamy K, Rasid MH, Jokhio GA, Budiea AMA, Hussin MW, Mirza J. Coal bottom ash as sand replacement in concrete: A review. *Constr Build Mater*. 2020;236:1–12. <https://doi.org/10.1016/j.conbuildmat.2019.117507>
- [14] Yao ZT, Ji XS, Sarker JK, Tanga JH, Ge LQ, Xia MS, et al. A comprehensive review on the applications of coal fly ash. *Earth Sci Rev*. 2015;141:105–21.
- [15] Abdullah MH, Rashid ASA, Anuar UHM, Marto A, Abuelgasim R. Bottom ash utilization: A review on engineering applications and environmental aspects. *IOP Conf Ser Mater Sci Eng*. 2019;527(1).
- [16] Basheer PAM, Bai Y. Strength and durability of concrete with ash aggregate. In: *Proceedings of the Institution of Civil Engineers Structures & Buildings*. 2005. p. 191–9.
- [17] Aggarwal P, Aggarwal Y, Gupta SM. Effect of bottom ash as replacement of fine aggregates in concrete. *Asian J Civ Eng (Building Housing)*. 2007;8(1):49–62.
- [18] Andrade LB, Rocha JC, Cheriaf M. Influence of coal bottom ash as fine aggregate on fresh properties of concrete. *Constr Build Mater*. 2009;23(2):609–14. <http://dx.doi.org/10.1016/j.conbuildmat.2008.05.003>
- [19] Siddique R, Aggarwal P, Aggarwal Y. Mechanical and durability properties of self-compacting concrete containing fly ash and bottom ash. *J Sustain Cem Mater*. 2012;1(3):67–82.
- [20] Abubakar AU, Baharudin KS. Potential Use Of Malaysian Thermal Power Plants Coal Bottom Ash In Construction. *Int J Sustain Constr Eng Technol*. 2012;3(2):25–37.
- [21] Al-fasih MYM, Ibrahim MHW, Basirun NF, Jaya RP, Sani MSHBM. Influence of partial replacement of cement and sand with coal bottom ash on concrete properties. *Int J Recent Technol Eng*. 2019;8(3S3):356–62.
- [22] Zhou H, Bhattarai R, Li Y, Si B, Dong X, Wang T, et al. Towards sustainable coal industry: Turning coal bottom ash into wealth. *Sci Total Environ*. 2022;804:149985.
- [23] Jatrapitakkul C, Cheerarot R. Development of bottom ash as pozzolanic material. *J Mater Civ Eng*. 2003;15(1):48–53.
- [24] Kim HK. Utilization of sieved and ground coal bottom ash powders as a coarse binder in high-strength mortar to improve workability. Vol. 91, *Construction and Building Materials*. 2015. p. 57–64.
- [25] Mangi SA, Ibrahim MHW, Jamaluddin N, Arshad MFa, Jaya RP. Short-term effects of sulphate and chloride on the concrete containing coal bottom ash as supplementary cementitious material. *Eng Sci Technol an Int J*. 2019;22(2):515–22. <https://doi.org/10.1016/j.jestch.2018.09.001>
- [26] Mangi SA, Wan Ibrahim MH, Jamaluddin N, Arshad MF, Memon SA, Shahidan S. Effects of grinding process on the properties of the coal bottom ash and cement paste. *J Eng Technol Sci*. 2019;51(1):1–13.
- [27] Mangi SA, Wan Ibrahim MH, Jamaluddin N, Arshad MF, Memon FA, Putra Jaya R, et al. A Review on Potential Use of Coal Bottom Ash as a Supplementary Cementing Material in Sustainable Concrete Construction. *Int J Integr Eng*. 2018;10(9):28–36.
- [28] Mangi SA, Ibrahim MHW, Jamaluddin N, Arshad MF, Memon SA, Shahidan S, et al. Coal bottom ash as a sustainable supplementary cementitious material for the concrete exposed to seawater. *AIP Conf Proc*. 2019;2119(July):1–8.

- [29] Argiz C, Moragues A, Menéndez E. Use of ground coal bottom ash as cement constituent in concretes exposed to chloride environments. *J Clean Prod.* 2018;170(January):25–33.
- [30] Brás A, Faustino P. Repair mortars and new concretes with coal bottom and biomass ashes using rheological optimisation. *Int J Environ Res.* 2016;10(2):203–16.
- [31] Khan RA, Ganesh A. The effect of coal bottom ash (CBA) on mechanical and durability characteristics of concrete. *J Build Mater Struct.* 2016;3(1):31–42. <http://journals.oasis-pubs.com>
- [32] Bajare D, Bumanis G, Upeniece L. Coal combustion bottom ash as microfiller with pozzolanic properties for traditional concrete. *Procedia Eng.* 2013;57:149–58. <http://dx.doi.org/10.1016/j.proeng.2013.04.022>
- [33] Martins IM, Gonçalves A. Durability and strength properties of concrete containing coal bottom ash. In: *International RILEM Conference on Material Science.* 2010. p. 6–10. <http://eprints.whiterose.ac.uk/76421/>
- [34] Ankur N, Singh N. Performance of cement mortars and concretes containing coal bottom ash: A comprehensive review. *Renew Sustain Energy Rev.* 2021;149(January):111361. <https://doi.org/10.1016/j.rser.2021.111361>
- [35] Behara NSR, Rao PS. Vibration energy harvesting using telescopic suspension system for conventional two-wheeler and EV. *Res Eng Struct Mater.* 2023;(March).
- [36] Singh N, Mithulraj M, Arya S. Influence of coal bottom ash as fine aggregates replacement on various properties of concretes: A review. *Resour Conserv Recycl.* 2018;138(July):257–71.
- [37] Singh N, Singh SP. Carbonation resistance of self-compacting recycled aggregate concretes with silica fume. *J Sustain Cem Mater.* 2018;7(4):214–38.
- [38] Cheah CB, Ramli M. Mechanical strength, durability and drying shrinkage of structural mortar containing HCWA as partial replacement of cement. *Constr Build Mater.* 2012;30:320–9. <http://dx.doi.org/10.1016/j.conbuildmat.2011.12.009>
- [39] Batt AS, Garg A. Partial Replacement of Wood Ash with Ordinary Portland Cement and Foundry Sand as Fine Aggregate. *J Civ Environ Eng.* 2017;07(02).
- [40] Singh N, Singh SP. Validation of Carbonation Behaviour of Self Compacting Concrete made with Recycled Aggregates using Microstructural and Crystallization Investigations. *Eur J Environ Civ Eng.* 2018;
- [41] Singh N, Shehnazdeep, Bhardwaj A. Reviewing the role of coal bottom ash as an alternative of cement. *Constr Build Mater.* 2020;233:117276. <https://doi.org/10.1016/j.conbuildmat.2019.11727>
- [42] Bai Y, Basheer PAM. Influence of furnace bottom ash on properties of concrete. In: *Proceedings of the Institution of Civil Engineers: Structures and Buildings.* 2003. p. 85–92.
- [43] Basheer PAM. Permeation analysis. In: *Handbook of analytical technology: principles, techniques and applications (Ramachandran V S and Beaudoin J J (eds)).* Noyes Publications, NJ,; 2001. p. 658–737.
- [44] Hussain M, Tufa LD, Yusup S, Zabiri H. Characterization of coal bottom ash & its potential to be used as catalyst in biomass gasification. In: *Materials Today: Proceedings.* 2019. p. 1886–93.
- [45] Kasemchaisiri R, Tangtermsirikul S. Properties of self-compacting concrete incorporating bottom ash as a partial replacement of fine aggregate. *ScienceAsia.* 2008;34(1):87–95.
- [46] Siddique R, Kunal. Design and development of self-compacting concrete made with coal bottom ash. *J Sustain Cem Mater.* 2015;4(3):225–37.
- [47] IS:8112-2013. IS 8112: 2013, Ordinary Portland Cement, 43 Grade — Specification, Bureau of Indian Standards, New Delhi. Bureau of Indian Standards, New Delhi. 2013.
- [48] IS 383: 2016. Coarse and fine aggregate for concrete - specification (third revision). Vol. third edit, Indian Standard. 2016.

- [49] IS 10262. Concrete Mix Proportioning Guidelines IS 10262. 2019.
- [50] Indian Standard. IS 516 - 1959 Methods of Tests for Strength of Concrete. 2006.
- [51] RILEM. CPC-18 Measurement of hardened concrete carbonation depth. *Mater Struct.* 1988 Nov;21(6):453–5.
- [52] Delf University of Technology. Sustainability Impact Metrics. <https://www.ecocostsvalue.com/>
- [53] Ali B, Qureshi LA, Khan SU. Flexural behavior of glass fiber-reinforced recycled aggregate concrete and its impact on the cost and carbon footprint of concrete pavement. *Constr Build Mater.* 2020;262:120820. <https://doi.org/10.1016/j.conbuildmat.2020.120820>
- [54] Momotaz H, Rahman MM, Karim MR, Zhuge Y, Ma X, Levett P. Comparative study on properties of kerb concrete made from recycled materials and related carbon footprint. *J Build Eng.* 2023;72(March).
- [55] Wang C, Chen B, Vo TL, Rezanian M. Mechanical anisotropy, rheology and carbon footprint of 3D printable concrete: A review. *J Build Eng.* 2023;76(June):107309. <https://doi.org/10.1016/j.jobe.2023.107309>
- [56] Li XJ, Xie WJ, Jim CY, Feng F. Holistic LCA evaluation of the carbon footprint of prefabricated concrete stairs. *J Clean Prod.* 2021;329(August):129621. <https://doi.org/10.1016/j.jclepro.2021.129621>
- [57] Elkhaldi I, Roziere E, Turcry P, Loukili A. Towards global indicator of durability performance and carbon footprint of clinker-slag-limestone cement-based concrete exposed to carbonation. *J Clean Prod.* 2022;380(P1):134876. <https://doi.org/10.1016/j.jclepro.2022.134876>
- [58] Yüksel I, Genç A. Properties of concrete containing nonground ash and slag as fine aggregate. *ACI Mater J.* 2007;104(4):303–9.
- [59] Balasubramaniam T, Thirugnanam GS. An experimental investigation on the mechanical properties of bottom ash concrete. *Indian J Sci Technol.* 2015;8(10):992–7.
- [60] Kou SC, Poon CS. Properties of concrete prepared with crushed fine stone, furnace bottom ash and fine recycled aggregate as fine aggregates. *Constr Build Mater.* 2009;23(8):2877–86. <http://dx.doi.org/10.1016/j.conbuildmat.2009.02.009>
- [61] Kim HK, Lee HK. Use of power plant bottom ash as fine and coarse aggregates in high-strength concrete. *Constr Build Mater.* 2011;25(2):1115–22. <http://dx.doi.org/10.1016/j.conbuildmat.2010.06.065>
- [62] Raju R, Paul MM, Aboobacker KA. Strength performance of concrete using bottom ash as fine aggregate. *Int J Res Eng Technol.* 2014;2(9):111–22.
- [63] Singh M, Siddique R. Effect of low-calcium coal bottom ash as fine aggregate on microstructure and properties of concrete. *ACI Mater J.* 2015 Sep 1;112(5):693–703.
- [64] Silva LA, Nahime BO, Lima EC, Akasaki JL, Reis IC. XRD investigation of cement pastes incorporating concrete floor polishing waste. *Ceramica.* 2020;66(380):373–8.
- [65] Aggarwal Y, Siddique R. Microstructure and properties of concrete using bottom ash and waste foundry sand as partial replacement of fine aggregates. *Constr Build Mater.* 2014;54:210–23. <http://dx.doi.org/10.1016/j.conbuildmat.2013.12.051>
- [66] Yasipourtehrani S, Strezov V, Bliznyukov S, Evans T. Investigation of thermal properties of blast furnace slag to improve process energy efficiency. *J Clean Prod.* 2017;149:137–45.
- [67] Saleh HM, El-Sheikh SM, Elshereafy EE, Essa AK. Mechanical and physical characterization of cement reinforced by iron slag and titanate nanofibers to produce advanced containment for radioactive waste. *Constr Build Mater.* 2019;200:135–45.
- [68] Govindarajan D, Gopalakrishnan R. Spectroscopic Studies on Indian Portland Cement Hydrated with Distilled Water and Sea Water. *Front Sci.* 2012;1(1):21–7.
- [69] Kontoleon F, Tsakiridis P, Marinos A, Katsiotis N, Kaloidas V, Katsioti M. Dry-grinded ultrafine cements hydration. Physicochemical and microstructural characterization. *Mater Res.* 2013;16(2):404–16.

- [70] Lo FC, Lee MG, Lo SL. Effect of coal ash and rice husk ash partial replacement in ordinary Portland cement on pervious concrete. *Constr Build Mater.* 2021;286:122947.
- [71] Hamzah AF, Ibrahim MHW, Jamaluddin N, Jaya RP, Arshad MF, Abidin NEZ. Nomograph of self-compacting concrete mix design incorporating coal bottom ash as partial replacement of fine aggregates. *J Eng Appl Sci.* 2016;11(7):1671–5.
- [72] Singh M, Siddique R. Strength properties and micro-structural properties of concrete containing coal bottom ash as partial replacement of fine aggregate. *Constr Build Mater.* 2014;50:246–56. <http://dx.doi.org/10.1016/j.conbuildmat.2013.09.026>
- [73] Singh M, Siddique R. Compressive strength, drying shrinkage and chemical resistance of concrete incorporating coal bottom ash as partial or total replacement of sand. *Constr Build Mater.* 2014;68:39–48. <http://dx.doi.org/10.1016/j.conbuildmat.2014.06.034>
- [74] Rafeizonooz M, Mirza J, Salim MR, Hussin MW, Khankhaje E. Investigation of coal bottom ash and fly ash in concrete as replacement for sand and cement. *Constr Build Mater.* 2016;116(July):15–24. <http://dx.doi.org/10.1016/j.conbuildmat.2016.04.080>
- [75] Majhi RK, Nayak AN. Properties of concrete incorporating coal fly ash and coal bottom ash. *J Inst Eng Ser A.* 2019;100(3):459–69. <https://doi.org/10.1007/s40030-019-00374-y>
- [76] Derringer G, Suich R. Simultaneous Optimization of Several Response Variables. 2018;4065.
- [77] Luesak P, Pitakaso R, Sethanan K, Golinska-Dawson P, Srichok T, Chokanat P. Multi-Objective Modified Differential Evolution Methods for the Optimal Parameters of Aluminum Friction Stir Welding Processes of AA6061-T6 and AA5083-H112. *Metals (Basel).* 2023;13(2).
- [78] To-on P, Wichapa N, Khanthirat W. A novel TOPSIS linear programming model based on response surface methodology for determining optimal mixture proportions of lightweight concrete blocks containing sugarcane bagasse ash. *Heliyon.* 2023;9(7):e17755. <https://doi.org/10.1016/j.heliyon.2023.e17755>
- [79] Hamada HM, Al-attar A, Shi J, Yahaya F, Al MS, Yousif ST. Optimization of sustainable concrete characteristics incorporating palm oil clinker and nano-palm oil fuel ash using response surface methodology. *Powder Technol.* 2023;413(August 2022):118054. <https://doi.org/10.1016/j.powtec.2022.118054>
- [80] Dahish HA, Almutairi AD. Case Studies in Construction Materials Effect of elevated temperatures on the compressive strength of nano-silica and nano-clay modified concretes using response surface methodology. *Case Stud Constr Mater.* 2023;18(January):e02032. <https://doi.org/10.1016/j.cscm.2023.e02032>
- [81] Waheed H, Hamcumpai K, Nuaklong P. Effect of graphene nanoplatelets on engineering properties of fly ash-based geopolymers containing crumb rubber and its optimization using response surface methodology. *J Build Eng.* 2023;75(March):107024. <https://doi.org/10.1016/j.jobe.2023.107024>
- [82] Peng Q, Chen B, Lu Q, Li K, Jin W. Effect of steel-waste PET hybrid fiber on properties of recycled aggregate concrete based on response surface methodology. *Constr Build Mater.* 2023;397(26):132448. <https://doi.org/10.1016/j.conbuildmat.2023.132448>
- [83] ISO 14044. Environmental management - Life Cycle Assessment: Requirements and Guidelines. Geneva, Switzerland; 2006.
- [84] ISO 14040. Environmental management - Life Cycle Assessment: Principles and Framework. Geneva, Switzerland; 2006.
- [85] European Commission-Joint Research Center. ILCD Handbook International Reference Life Cycle Data System. Constraints. 2010. 1–393 p.